Journal of Science and Technology in Civil Engineering, HUCE, 2024, 18 (1): 143–152

ENERGY EVOLUTION OF GRAVITATIONAL-GRANULAR FLOWS

Quach Viet Anh[a], Nguyen Duc Manh[a], Le Van Thao[b], Vo Thanh Trung[c,d,*]

[a]*Faculty of Hydraulic Engineering, Hanoi University of Civil Engineering, 55 Giai Phong road, Hai Ba Trung district, Hanoi, Vietnam*
[b]*Faculty of Water Resources Engineering, University of Science and Technology - The University of Danang, 54 Nguyen Luong Bang street, Lien Chieu district, Da Nang city, Vietnam*
[c]*School of Transportation Engineering, Danang Architecture University, 566 Nui Thanh street, Da Nang city, Vietnam*
[d]*Office of Research Administration, Danang Architecture University, 566 Nui Thanh street, Da Nang city, Vietnam*

Article history:
Received 17/10/2023, Revised 14/3/2024, Accepted 20/3/2024

Abstract

The catastrophe of natural disasters such as landslides, is a prevalent phenomenon in natural terrain conditions in high mountainous areas; however, the mobility of such landslides has not yet well understood due to the discrete nature of material and the coming to play of water. In this paper, we numerically study the mobility of an unsaturated gravitational-granular flow, occurring on a slope-break system that contains two regions: inclined-upstream and horizontal-downstream areas, by using three-dimensional discrete element simulations. A sliding volume composed of spherical grains collapses on the first region, then plunges and deposits on the second one. The upstream-plunging length and the cohesive stress exerted on grains affect differently on the energy evolution not only in the whole process but also in different regions and directions depending on the inclination angle. These findings provide a deep understanding of the mechanism and mobility of landslides, leading to good predictions about the potential impacts of the catastrophic landslides on buildings and human lives.

Keywords: cohesive stress; discrete element method; flow mobility; kinetic energy; plunging length.

https://doi.org/10.31814/stce.huce2024-18(1)-11

1. Introduction

Landslides are a common natural phenomenon in high mountainous areas [1–4]. Due to the gravitational effects, configurations, and material properties, such natural events commonly generate large kinetic energy and seriously impact building and human lives [5–8]. However, our understanding of the characteristics and mobility of such gravitational-granular flows arising from these landslides, especially unsaturated soil conditions, is still very limited due to the difficulty in performing and measuring large experiments.

To comprehensively understand and predict the characteristics and mobility of landslides, a numerical experiment is well-known as an effective method. Different numerical methods such as Material Point Method (MPM) [9, 10], Smooth Particle Hydrodynamics (SPH) [11–13], and Discrete Element Method (DEM) [14, 15] have been used for simulating landslides. DEM model is well known as an initial step for investigating and confirming the flow mobility of granular materials because this method has the advantage of easily considering the particle size distribution, changing the grain properties and model configurations, as well as assessing the microscopic properties to demonstrate the

*Corresponding author. *E-mail address:* trungvt@dau.edu.vn (Trung, V. T.)

origins of macroscopic properties [16, 17]. Indeed, by using DEM, different effects of slope morphology, aspect ratio, column thickness, and sliding volume of material on the flow mobility of granular materials have been investigated and explained [18–22].

However, most of the previous studies on flow mobility are mainly concerned with dry materials, without varying slope angles and changing plunging lengths. As a result, it is difficult to get a better understanding of the mobility of granular materials. Recently, Vo and co-workers [15] numerically investigated the effects of slope angle and volume of material on the mobility of gravitational-granular flows utilizing the discrete element method. The results showed that the slope angle strongly affects the mobility of granular flows whereas the sliding volume slightly modifies the energy evolution, and a nice correlation between the runout distance and kinetic energy was introduced [15]. The findings provided evidence for getting a better understanding of the flow mobility of granular materials on a slope-break surface, however, the effects of the plunging length in the upstream region and the cohesive stress between grains should be also studied.

In this paper, we further study the granular flow's mobility by analyzing its energy evolution, during the whole process and also in different directions and different regions by investigating the effects of the upstream-plunging length and the cohesive stress between grains. Results obtained from this research show that the kinetic energy of the flow increases simultaneously with the upstream-plunging length, whereas the cohesive stress between the core particles material tends to reduce the average kinetic energy of the flow. It is remarkable to see that the kinetic energy in the whole process, in the vertical directions of the upstream region, and horizontal one of downstream area can be introduced almost as a nearly linear function of the slope angle for different values of the upstream plunging length. The results are expected to initially predict the dependences of the energy evolution of the granular flows on the upstream-plunging length, cohesive stress, and inclination angle, leading to complementing a better understanding of the mobility of unsaturated granular flows on complex surfaces, and providing a basis for making more accurate predictions about the characteristics of landslide flows as well as good bases for conducting research on landslides at different rates and phases of flow.

2. Numerical simulation and parameters

The simulations are performed based on the theory of discrete element method, where the position of the particles and the component forces are continuously being calculated and updated by the Newton's second law. Thanks to that, this numerical approach has been proved to be suitable for investigating the granular material in general and granular flow in particular.

In this ongoing work, we use a code program which named cFGdFlow-3D, originally developed by Patrick Mutabaruka and his colleagues [23]. This coding program is continuously getting updates and being improved by Vo Thanh Trung in order to apply different configurations of simulations for granular material [24, 25], including the one in this current paper. Firstly, the grains are modeled as rigid bodies and they can interact with others by considering the solid interaction forces and liquid forces [26]. As an example, we consider a

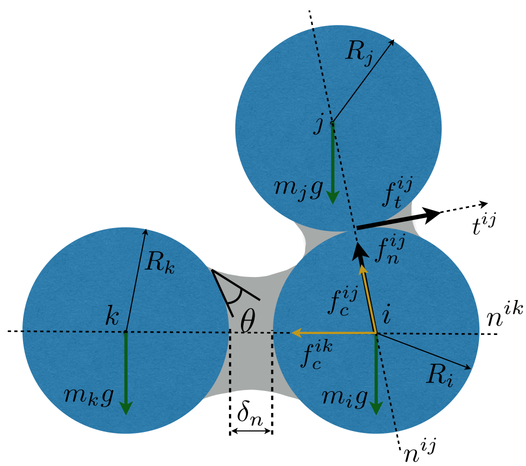

Figure 1. A schematic drawing representation the interactions between three particles *i*, *j*, and *k*

case of three primary wet particles (as shown in Fig. 1), particle i can interact with particle j via both solid and capillary contact, meanwhile, particle i only interacts with particle k via a capillary bond. A solid interaction contact can be characterized by the normal contact force f_n and the tangential contact force f_t, a capillary contact can be characterized by the capillary cohesive force f_c. f_n is well-known as a sum of the normal elastic force and normal damping component, f_t is obtained by considering the Coulomb friction law, and the cohesive force f_c is calculated via the liquid-vapor surface tension γ_s, obtained via the cohesion pre-factor $\kappa = 2\pi\gamma_s$ [27]. Therefore, the movement equation of particle i with radius $\mathbf{R_i}$ and mass $\mathbf{m_i}$ in the program will be:

$$m_i \frac{d^2 \boldsymbol{s}_i}{dt^2} = \sum \left\{ \left(f_n^{ij} + f_c^{ij} \right) n^{ij} + f_t^{ij} t^{ij} \right\} + \sum f_c^{ik} n^{ik} + m_i g \tag{1}$$

where $\boldsymbol{s}_i$ is the position vector of grain i; $\boldsymbol{n}$ and $\boldsymbol{t}$ are the normal unit vector and tangential unit vector between two particles in contact. In which, $\boldsymbol{n}$ is perpendicular to the contact plane between particle i and j ($\boldsymbol{n}^{ij}$) or between particle i and k ($\boldsymbol{n}^{ik}$), $\boldsymbol{t}$ has the direction opposite to the relative tangential displacement between particle i and j ($\boldsymbol{t}^{ij}$).

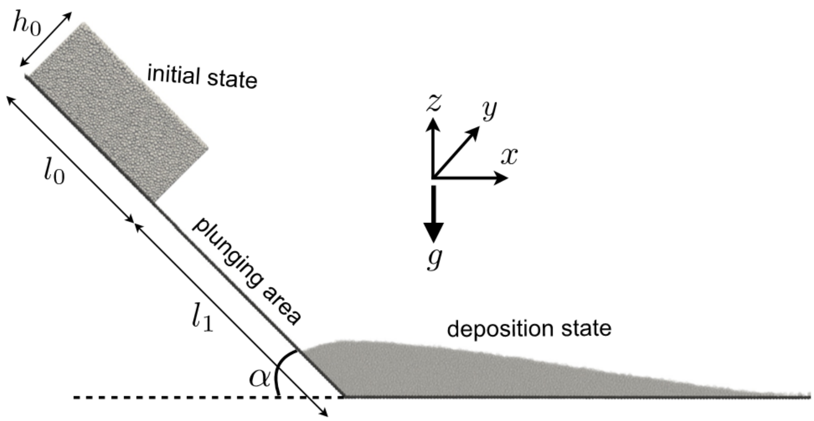

Figure 2. Collapse model of a sliding volume on a slope-break surface in $x - z$ view

Subsequently, the current work is prepared and simulated via four different stages:

1) Creating a sliding volume by a package of primary particles putting randomly in a rectangular box.

2) Applying an isotropic compression on all six sides of the box until reaching a dense configuration.

3) Putting this configuration at the top of the inclined upstream region then releasing all the walls of the box except for the two restrictions on the x-direction. The rough surfaces of the upstream and downstream region are created by gluing particles that have the same shape, size, and mass. The size of these particles is equivalent to the mean particle diameter ($\langle d \rangle \approx 1.2$ mm) modelled in the granular assembly. These particles are arrayed and immobilized during the collapse process of granular materials. The definition of this failure surface can partly reflect the phenomenon of granular flows down in reality.

4) Releasing the front wall in the x-direction. The particles will be moved under the gravitational force and create a granular flow on a slope-break surface.

Concerning the particles' diameters, by setting them to be distributed uniformly from the smallest $d_{\min}$ to the largest size $d_{\max}$ with a correlation that $d_{\max}/d_{\min} = 2$, this distribution can avoid the crystallization effects in granular media, implying to prevent particles arrangement as ordered structures. In this study, we only use one case of the particle size distribution. Subsequently, the slope angle is continuously varied in a wide range from 25° to 60°, these values of the slope angle exceed the angle of repose of modeled granular material, also reflects the most common cases of sliding angle on mountainous area [15]. In terms of the sliding volume's dimensions, the initial height h_0 is fixed at 0.0290 m, while the initial length l_0 of the box is declared by the author. As reported by Zhang et al. [19] when considering the collapse dynamics and deposition morphology of granular columns on a horizontal plane, the increase of the column's thickness leads to an increase of the kinetic energy of the flows, implying that the use of two-dimensional (2D) or three-dimensional (3D) model affects the flow mobility of granular materials. Concerning the expectations of predicting the mobility of landslides in the current paper and limitations of the DEM simulations, a 3D model is preferably considered with a not-too-large width of the model, fixed closely to 17.5 times the mean particle diameter $\langle d \rangle$. We choose two different values of l_0 (0.0550 m and 0.0653 m), corresponding to two volume cases, representing two different numbers of primary particles (25,752; 30,420). In our current work, three plunging lengths of the inclined surface $l_1 = \{0.10; 0.15; 0.20\}$ m and four other cases of cohesive stress $\sigma_c = \{0.0; 41.7; 83.3; 187.5\}$ N/m^2 are used for considering their impact on the mobility of the granular flow.

The material properties used in the current work are chosen as a common case of granular materials normally modelled at particle-scale level by the discrete element method to investigate the energy evolution during the collapse and deposition of granular columns. Indeed, Wu et al. [28] used a small-scale numerical model to predict the flow mobility and runout behavior of granular materials, this was also nicely validated with an experimental work. In our ongoing work, the numerical model extends our previous investigation [15], this is also validated with a theoretical analysis. Our previous results confirm that the DEM simulations can well predict flow mobilities and runout distance of granular flows. In which, the normal stiffness or grains took the prevalent value of 10^6 Nm^{-1}, whereas the tangential stiffness constitutes 80% of normal stiffness. Meanwhile, the tangential damping and normal damping are equal $\gamma_\mathrm{n} = \gamma_\mathrm{t} = 0.5$ Nsm^{-1}. As a consequence of choosing these values, the normal and tangential deflection is imposed to be approximately 10^{-3} times with the mean diameter of two grains in contact and the dynamic part of the flow is expressed. The time step t is chosen to be small enough to capture all the changes of the energy evolution. In summary, we list the principal parameters and their values in the Table 1.

Table 1. Main parameters used in all simulations

Parameter	Symbol	Value	Unit
Largest particle diameter	$\mathrm{d}_{\mathrm{max}}$	1.6	mm
Particles' density	ρ	2600	kg m^{-3}
Coefficient of friction	μ	0.3	-
Normal stiffness	k_n	10^6	N/m
Tangential stiffness	k_t	8×10^5	N/m
Normal damping	γ_n	0.5	Ns/m
Tangential damping	γ_t	0.5	Ns/m
Inclination angle	α	[25,60]	°
Cohesive stress	σ_c	{0,187.5}	N/m^2
Plunging length	l_1	{0.10; 0.15; 0.20}	m
Time step	Δt	1.2×10^{-7}	sec.

3. Results and discussions

The mobility of gravitational-granular flow, expressed by its energy evolution, is greatly impacted by not only the sliding volume's parameters such as the volume of the sliding block (or could be understood as the length of the box l_0 that grows as the number of the grains increases) and the cohesive stress between particles (σ_c), but also the characteristics of the upstream region via the inclination angle and plunging length of this surface.

To commence, we study the effect of changing these parameters on the normalized kinetic energy of the whole system. The mean value of the kinetic energy $\langle E \rangle$ is normalized by the initial average potential energy of the grains $\left\langle E_p \right\rangle$ in the sliding volume. Fig. 3 displays the evolution of kinetic energy of the landslide at different normalized time instants t/t_c, which t_c is a constant value that denotes the time required for a particle with average diameter $\langle d \rangle$ to fall vertically a distance $\langle d \rangle$ under the effect of gravity, for different cases of study (noted under the figures), where the symbol $\langle \ldots \rangle$ will represent the calculation of a mean. Overall, both plots in Fig. 3 share the same tendency where the kinetic energy starts from the repose status, then climbs rapidly to reach a peak of value $\langle E \rangle_{\max}$, followed by a sharp decrease and finally gradually declines back to the deposition stage.

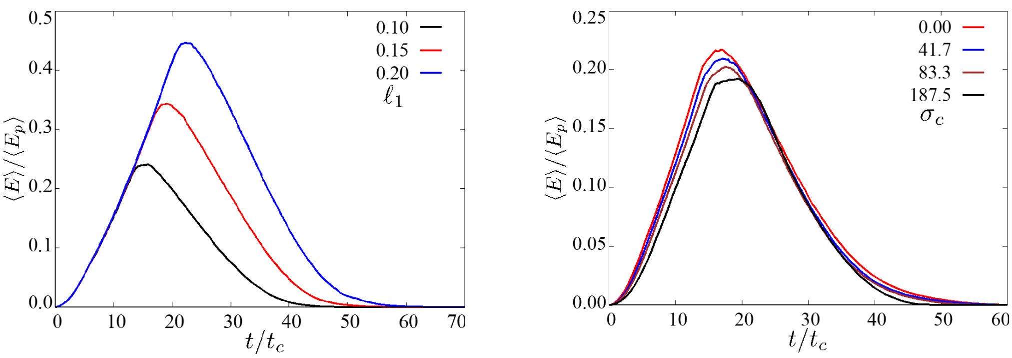

(a) $l_0 = 0.0550m$, $\alpha = 45°$ (b) $l_0 = 0.0653m$, $\alpha = 40°$

Figure 3. Normalized kinetic energy of the granular block collapses on a rigid granular surface by considering different parameters

In particular, Fig 3(a) demonstrates the effects of the upstream-plunging length on the flow mobility of granular materials. Remarkably, the rate of increasing the normalized kinetic energy is the same when the upstream-plunging length is varied. However, the peak value of the normalized kinetic energy increases with increasing the lunging length of the upstream area, implying that the larger upstream-plunging length leads to higher kinetic energy. Interestingly, after reaching the peak, the declining rate of both lines seems to be dependent on the plunging length.

Contrary to the effects of the upstream-plunging length, the cohesive stress between grains leads to reduction the kinetic energy of the flows. Indeed, Fig. 3(b) considers the evolution of the normalized kinetic energy in the whole collapse process as a function of the normalized collapse time by changing the cohesive stress exerted on each grain. These observations confirm the cohesive effects of material in nature, this cohesive stress surely helps to decrease the kinetic energy of the granular flow in landslides. Indeed, the rate to climb to the peak and its value witness a gradually decline, opposed to the raise of cohesive component.

Besides the kinetic energy of the whole process, it is still fundamental to investigate its smaller components, dividing by directions and by regions, which are in vertical $\left\langle E_z^u \right\rangle$ and horizontal $\langle E_x^u \rangle$ in upstream region, and vertical $\left\langle E_z^d \right\rangle$ and horizontal $\left\langle E_x^d \right\rangle$ in downstream region in order to represent the energy evolution. Consequently, we could now study the dependence of the mobility of the landslide flow on each element of the four parameters that we are changing.

Fig. 4 displays the correlation between the normalized kinetic energy on upstream $\left(\left\langle E_z^u\right\rangle, \langle E_x^u\rangle\right)$ and downstream $\left(\left\langle E_z^d\right\rangle, \left\langle E_x^d\right\rangle\right)$ areas, in vertical and horizontal directions, respectively, as a function of the normalized collapse time for three value of the upstream-lunging length l_1 while fixing the sliding block's volume and the inclination angle (45°). Similarly, these graphs share the same trend which belongs to the mean kinetic energy of the whole process $\langle E\rangle$ when they climb to hit the highest point then decline back to zero. Through these charts, we could be certain that the rate of occurring to the highest value of energy and the decreasing rate to the stable status are nearly independence of the plunging length. On the contrary, this factor makes the highest value of components of kinetic energy higher and longer to achieve when it increases.

In order to analyze the influences of the cohesion of wet granules on the kinetic energies on both regions, we keep the sliding volume, inclination angle and plunging length of the inclined plane unchanged as in Fig. 5. Sharing the same trend with ⟨E⟩, the value of $\left\langle E_z^u\right\rangle$, $\langle E_x^u\rangle$, $\left\langle E_z^d\right\rangle$ and $\left\langle E_x^d\right\rangle$ initially witness a staggering increase, but their maximum value and their rate to go up seem to fall according to the growth of the cohesive force. Nevertheless, the drier granular material, the more time it takes the modelization to finish the depositing process.

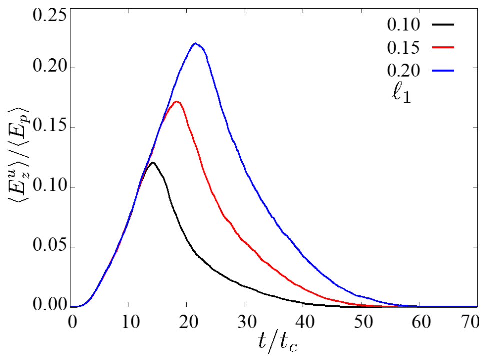

(a) Normalized vertical kinetic energy on upstream region

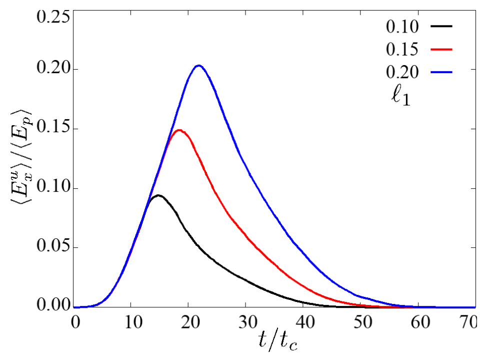

(b) Normalized horizontal kinetic energy on upstream region

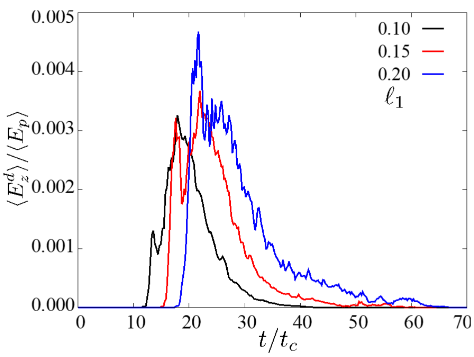

(c) Normalized vertical kinetic energy on downstream region

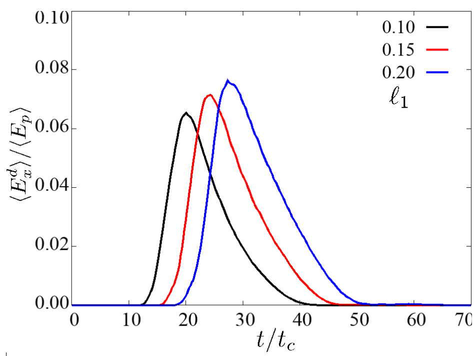

(d) Normalized horizontal kinetic energy on downstream region

Figure 4. Evolution of different normalized kinetic energies as a function of the normalized collapse time for three values of the upstream length l_1 with a given value $l_0 = 0.0550$ m and $\alpha = 45°$

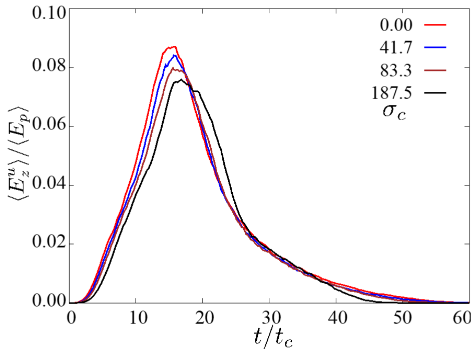

(a) Normalized vertical kinetic energy on upstream region

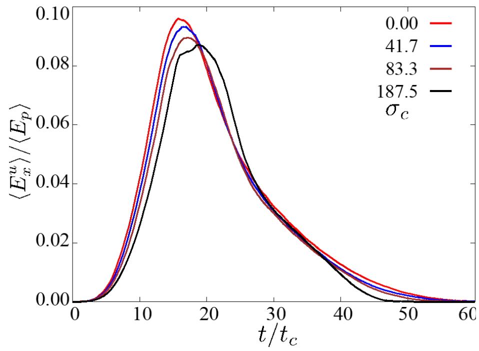

(b) Normalized horizontal kinetic energy on upstream region

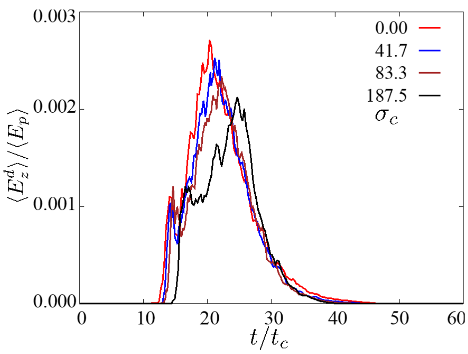

(c) Normalized vertical kinetic energy on downstream region

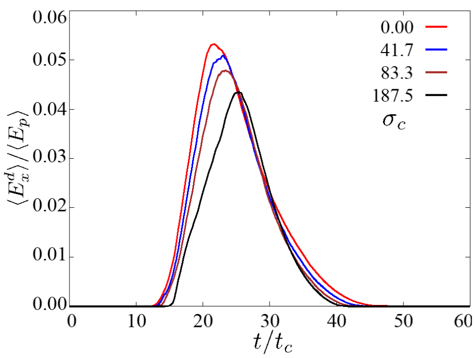

(d) Normalized horizontal kinetic energy on downstream region

Figure 5. Evolution of different normalized kinetic energies as a function of the normalized collapse time for three values of the cohesive stress σ_c with a given value $l_0 = 0.0653$ m, $l_1 = 0.1$ m, and $\alpha = 40°$

In order to comprehensively highlight the effects of the upstream-plunging length l_1 on the evolution of kinetic energy of landslide flows with different slope angles α, the relation between l_1 and the maximum value of the normalized mean kinetic energy in the whole process and in different regions and directions are considered, as shown in Fig. 6 and Fig. 7, respectively.

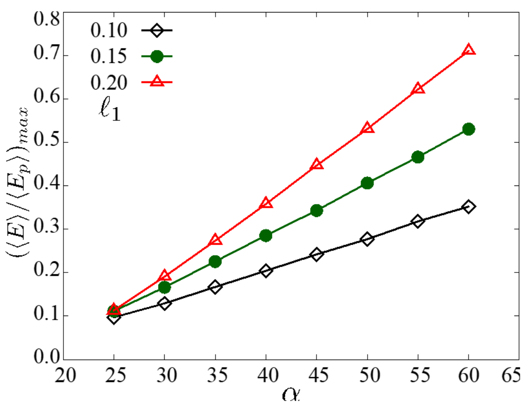

Figure 6. Evolution of $\left(\langle E \rangle / \langle E_p \rangle\right)_{\max}$ as a function of the slope angle for three values of the plunging length l_1 with a given value $l_0 = 0.0550$ m for dry granular materials

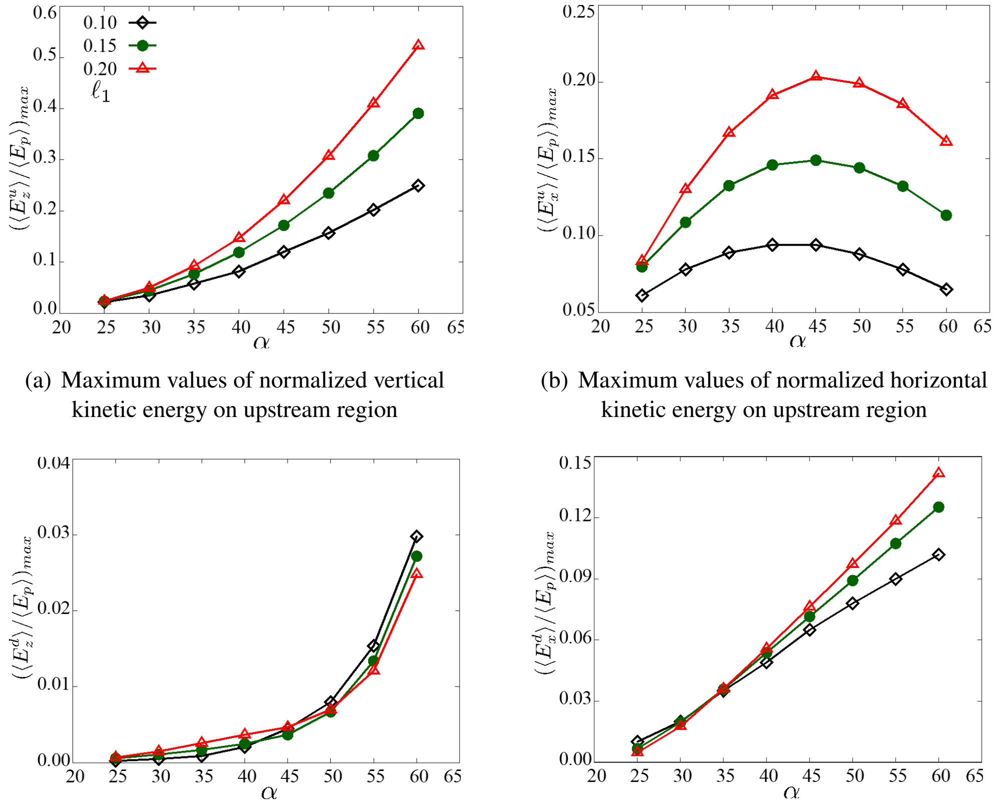

(a) Maximum values of normalized vertical kinetic energy on upstream region

(b) Maximum values of normalized horizontal kinetic energy on upstream region

(c) Maximum values of normalized vertical kinetic energy on downstream region

(d) Maximum values of normalized horizontal kinetic energy on downstream region

Figure 7. Maximum values of different normalized kinetic energies as a function of α for three values of the plunging length l_1 with a given value l_0 = 0.0550 m for noncohesive granular materials

As being shown in Fig. 6, the values of $\left(\langle E \rangle / \langle E_p \rangle\right)_{\max}$ increase nearly linear with α for all cases of l_1, but with the rate that increases with increasing the upstream-plunging length. In particular, the upstream-plunging length l_1 slightly affects the peak value of kinetic energy for lower slope surface but significantly governs this energy for higher slope angle. These findings clearly provide a good understanding of the evolution of kinetic energy increased during the landslide flows with different cases of the terrain slope angle and the upstream-plunging length.

Most of the other components of kinetic energy share the same tendency with $\left(\langle E \rangle / \langle E_p \rangle\right)_{\max}$ as they raise simultaneously with the increase of α and l_1. A quite similar presentation of $\left(\langle E_z^u \rangle / \langle E_p \rangle\right)_{\max}$ and $\left(\langle E_x^d \rangle / \langle E_p \rangle\right)_{\max}$ in Fig. 7 with $\left(\langle E \rangle / \langle E_p \rangle\right)_{\max}$ in Fig. 6 is recorded, as they express almost as a linear function. The nonlinear phenomenon of $\left(\langle E_x^u \rangle / \langle E_p \rangle\right)_{\max}$ and $\left(\langle E_z^d \rangle / \langle E_p \rangle\right)_{\max}$, respectively shown in Figs. 7(b) and (c), may be well explained due to the strong transformation of energy from the vertical direction to the horizontal one in the heap stage as a consequence of changing the slope angle. Remarkably, the effects of α manifests un-similarly with the others on the normalized horizontal kinetic energy on upstream area, as shown in Fig. 7(b). In particular, $\left(\langle E_z^u \rangle / \langle E_p \rangle\right)_{\max}$ first soars to the highest value when the slope angle is increased up to about 45°, then suddenly plummets from this point on to the higher value of inclination angle. These observations clearly show the physical behavior of common gravitational-granular flows occurred in landslide events in mountainous areas or near the hydraulic constructions.

4. Conclusions

Through this paper, we have studied the influence of the sliding inclination angle, upstream-plunging length, and cohesive stress exerted on each grain on the movement characteristics of the flow of granular materials utilizing the discrete element method. Results obtained from the model show that the inclination angle of the sliding surface and the length of the upstream sliding zone have different influences on the energy evolution of the flow, while the cohesive stress between the particles tends to reduce the average kinetic energy. It is worth to remark that the maximum normalized average kinetic energy of the whole process, and the normalized average kinetic energy value in the vertical and horizontal directions respectively in the upstream and downstream surfaces are expressed as different functions of the inclination angles, correspond to different values of the upstream plunging length. This leads to providing evidence for predicting the evolution and magnitude of kinetic energy according to different conditions of the sliding surface and material properties in reality.

Although the findings observed in this current work show the detailed influence of the inclination angle, upstream-plunging length, and cohesive stress on the energy evolution of gravitational-granular flows, these numerical results were only obtained for common cases of material properties used in DEM instead of considering real granular materials, without considering the pore water pressure, the effects of interparticle friction coefficient and particle shape, or fixing the failure angle during the process. These assumptions may lead to the slight influence on the mobility of granular flows.

Acknowledgements

This research is funded by Vietnam National Foundation for Science and Technology Development (NAFOSTED) under grant number 107.01-2021.23.

The authors gratefully acknowledge Dr. Nguyen Trung Kien, Dr. Tran Dinh Minh, and Dr. Nguyen Thanh Hai for their fruitful discussions.

References

[1] Iverson, R. M. (2015). Scaling and design of landslide and debris-flow experiments. *Geomorphology*, 244:9–20.

[2] Gariano, S. L., Guzzetti, F. (2016). Landslides in a changing climate. *Earth-Science Reviews*, 162: 227–252.

[3] Van Tien, P., Luong, L. H., Duc, D. M., Trinh, P. T., Quynh, D. T., Lan, N. C., Thuy, D. T., Phi, N. Q., Cuong, T. Q., Dang, K., Loi, D. H. (2021). Rainfall-induced catastrophic landslide in Quang Tri Province: the deadliest single landslide event in Vietnam in 2020. *Landslides*, 18:2323–2327.

[4] Huggel, C., Korup, O., Gruber, S. (2022). *Landslide Hazards and Climate Change in High Mountains*. Elsevier, 798–814.

[5] He, J., Zhang, L., Xiao, T., Chen, C. (2022). Emergency risk management for landslide dam breaks in 2018 on the Yangtze River, China. *Resilient Cities and Structures*, 1(3):1–11.

[6] Ahmed, S., Liquin, P. (2023). Socio-ecological challenges of hydroelectric dams among ethnic minorities in northern Laos. *Environmental Development*, 46:100864.

[7] Evans, S. G. (1989). The 1946 Mount Colonel Foster rock avalanche and associated displacement wave, Vancouver Island, British Columbia. *Canadian Geotechnical Journal*, 26(3):447–452.

[8] Fritz, H. M., Mohammed, F., Yoo, J. (2009). *Lituya Bay Landslide Impact Generated Mega-Tsunami 50th Anniversary*. Birkhäuser Basel, 153–175.

[9] Andersen, S., Andersen, L. (2009). Modelling of landslides with the material-point method. *Computational Geosciences*, 14(1):137–147.

[10] Zhao, L., Qiao, N., Huang, D., Zuo, S., Zhang, Z. (2022). Numerical investigation of the failure mechanisms of soil–rock mixture slopes by material point method. *Computers and Geotechnics*, 150:104898.

[11] Nguyen, C. T., Nguyen, C. T., Bui, H. H., Nguyen, G. D., Fukagawa, R. (2016). A new SPH-based approach to simulation of granular flows using viscous damping and stress regularisation. *Landslides*, 14 (1):69–81.

[12] Zhang, Z., Jin, X., Bi, J. (2019). Development of an SPH-based method to simulate the progressive failure of cohesive soil slope. *Environmental Earth Sciences*, 78(17).

[13] Bui, H. H., Nguyen, G. D. (2021). Smoothed particle hydrodynamics (SPH) and its applications in geomechanics: From solid fracture to granular behaviour and multiphase flows in porous media. *Computers and Geotechnics*, 138:104315.

[14] Nguyen, N. H. T., Bui, H. H., Nguyen, G. D. (2020). Effects of material properties on the mobility of granular flow. *Granular Matter*, 22(3).

[15] Vo, T.-T., Tran, D. M., Nguyen, C. T., Nguyen, T.-K. (2023). Discrete element investigation of the mobility of granular mass flows. *Solid State Communications*, 369:115190.

[16] Vo, T.-T., Nguyen, C. T., Nguyen, T.-K., Nguyen, V. M., Vu, T. L. (2022). Impact dynamics and power-law scaling behavior of wet agglomerates. *Computational Particle Mechanics*, 9(3):537–550.

[17] Vo, T.-T., Nguyen, T.-K. (2023). Insights into the compressive and tensile strengths of viscocohesive–frictional particle agglomerates. *Computational Particle Mechanics*, 10(6):1977–1987.

[18] Daudon, D., Villard, P., Richefeu, V., Mollon, G. (2014). Influence of the morphology of slope and blocks on the energy dissipations in a rock avalanche. *Comptes Rendus. Mécanique*, 343(2):166–177.

[19] Zhang, R., Su, D., Lei, G., Chen, X. (2021). Three-dimensional granular column collapse: Impact of column thickness. *Powder Technology*, 389:328–338.

[20] Man, T., Huppert, H. E., Li, L., Galindo-Torres, S. A. (2021). Deposition morphology of granular column collapses. *Granular Matter*, 23(3).

[21] Cagnoli, B. (2021). Stress level effect on mobility of dry granular flows of angular rock fragments. *Landslides*, 18(9):3085–3099.

[22] Li, K., Wang, Y., Cheng, Q., Lin, Q., Wu, Y., Long, Y. (2022). Insight Into Granular Flow Dynamics Relying on Basal Stress Measurements: From Experimental Flume Tests. *Journal of Geophysical Research: Solid Earth*, 127(3).

[23] Mutabaruka, P. (2013). Numerical modeling of immersed granular media: initiation and propagation of avalanches in a fluid. PhD thesis, Université de Montpellier.

[24] Vo, T. T., Nezamabadi, S., Mutabaruka, P., Delenne, J.-Y., Radjai, F. (2020). Additive rheology of complex granular flows. *Nature Communications*, 11(1).

[25] Vo, T.-T., Nguyen, T.-K. (2023). Moving intruder out of noncohesive and cohesive granular assemblies. *Computational Particle Mechanics*, 10(5):1005–1017.

[26] Radjai, F., Dubois, F. (2011). *Discrete-element modeling of granular materials*. Wiley-Iste.

[27] Vo, T.-T., Nguyen, C. T. (2021). Characteristics of force transmission in cohesive agglomerates impacting a rigid surface. *Mechanics Research Communications*, 117:103773.

[28] Wu, Y., Sun, Y., Wang, D. (2023). The combined effect of cohesion and finite size on the collapse of wet granular columns. *Soft Matter*, 19(48):9520–9530.